Deep-Sea Research Part II 164 (2019) 5–13

Contents lists available at ScienceDirect

Deep-Sea Research Part II

journal homepage: www.elsevier.com/locate/dsr2

The effect of wind-stress over the Eastern Mediterranean on deep-water formation in the Adriatic Sea

Yael Amitai[a,*], Yosef Ashkenazy[b], Hezi Gildor[a]

[a] The Institute of Earth Sciences, The Hebrew University of Jerusalem, Edmond J. Safra Campus, Givat Ram, Jerusalem 91904, Israel
[b] Solar Energy and Environmental Physics, BIDR, Ben-Gurion University of the Negev, Sede Boqer Campus, 84990 Midreshet Ben-Gurion, Israel

ARTICLE INFO

Keywords:
Levantine intermediate water
Adriatic deep water formation
Eastern Mediterranean

ABSTRACT

We investigate the effect of interannual variability of the wind-stress over the Eastern Mediterranean on Adriatic Deep Water (ADW) formation using an oceanic general circulation model of the Mediterranean Sea driven by monthly ERA-Interim wind-stress of the years 1979–2014. This is done by using climatological annual cycle of the surface temperature and freshwater flux but interannually varying wind-stress.

A connection between the wind-stress magnitude over the Rhodes Gyre region and ADW outflow is found in association with the formation of Levantine Intermediate Water (LIW). 720 years artificially generated wind-stress fields were constructed based on the first 50 Empirical Orthogonal Functions (EOFs) of the wind-stress monthly anomalies. This simulation strengthen the connection that was found and also reveal a centennial internal variability of both the LIW and the ADW outflow.

It is also found that the intensity of the Rhodes Gyre is almost linearly related to the wind-stress amplitude. However, the ADW outflow is non-monotonically related to the wind-stress amplitude. There is an optimal wind-stress amplitude for which the ADW formation is maximal. When the wind-stress amplitude is more than 50% the climatological mean wind-stress amplitude, the ADW outflow is weakened. This implies a different balance between the saline LIW and the fresh Atlantic Water, entering the Eastern Mediterranean from Sicily Strait, under stronger than present wind-stress amplitude.

1. Introduction

The Adriatic, an elongated, semi-enclosed Sea is historically recognized as the primary deep water source of the Eastern Mediterranean (EM). Even though a transient source of deep water was reported in the Aegean Sea during 1987–1995, known as the Eastern Mediterranean Transient (EMT; Roether et al., 1996; Klein et al., 1999), the Adriatic Sea returned to act as the main EM deep water provider afterward (Klein et al., 2000; Manca et al., 2003). Adriatic Deep Water (ADW) formation occurs as either open ocean convection in the vicinity of the south-Adriatic pit (~1200 m; Ovchinnikov et al., 1985; Mantziafou and Lascaratos, 2004) or as a shelf convection over the Adriatic continental shelf (Artegiani et al., 1997a; Chiggiato et al., 2016). The ADW outflows through the Otranto Strait in an average rate of ~0.3 Sv ($1\,\mathrm{Sv} \equiv 10^6 \mathrm{m^3 s^{-1}}$) and is characterized by a density exceeding 29.2 $\sigma_\theta\,[kg/m^3]$, filling the abyss of the Ionian Sea (Malanotte-Rizzoli et al., 1997). The ADW outflow exhibits a large seasonal and interannul variability (Russo and Artegiani, 1996; Mantziafou and Lascaratos, 2004; Cardin et al., 2011, 2015), which is attributed to both intense surface heat loss and to a salinity preconditioning (Manca et al., 2003; Mantziafou and Lascaratos, 2008; Verri et al., 2018) imposed by the incoming Levantine Intermediate Water (LIW). Malanotte-Rizzoli et al. (1999) showed that the transition to an active source of deep water in the Aegean was a consequence of a three-lobe anticyclonic structure blocking the LIW flow into the Ionian, causing it to recirculate in the Levantine and eventually to flow to the Aegean instead. Amitai et al. (2017) showed that ADW formation has multiple equilibria under present-day like conditions and that the state of a ceased ADW outflow is caused by reduced saline LIW flowing from the Aegean Sea region into the Adriatic Sea.

In the climatological flow pattern LIW forms at the surface, from Atlantic Water (AW) that evaporate while propagating eastward, and sinks to intermediate depths (200–700 m). This happens primarily in the Rhodes Gyre area, but also, to some extent, in other areas of the Levantine basin (Ovchinnikov and Plakhin, 1984; Robinson et al., 1992; Lascaratos et al., 1993; Wu and Haines, 1996; Vervatis et al., 2013). The Rhodes Gyre is a well documented gyre that is known as an EM permanent circulation feature that is induced by wind-stress curl (Pinardi

* Corresponding author.
E-mail addresses: yael.amitai@mail.huji.ac.il (Y. Amitai), ashkena@bgu.ac.il (Y. Ashkenazy), hezi.gildor@huji.ac.il (H. Gildor).

https://doi.org/10.1016/j.dsr2.2018.11.015

Available online 24 November 2018
0967-0645/ © 2018 Elsevier Ltd. All rights reserved.

and Navarra, 1993; Korres et al., 2000; Molcard et al., 2002; Pinardi et al., 2015).

After forming, the LIW is advected through the Cretan passage to the Northern Ionian intermediate layer (among other regions of the EM) and a portion of it flows into the Adriatic Sea. Its importance for ADW formation processes was evident, for example, in triggering the recovery of the Adriatic source after the EMT (Klein et al., 2000; Manca et al., 2003). Furthermore, eddy resolving simulations of the Adriatic Sea indicate that the saline LIW is a key factor in ADW formation process (Oddo and Guarnieri, 2011; Gunduz et al., 2013; Querin et al., 2013).

Gačić et al. (2010) proposed the Adriatic-Ionian Bimodal-OScillation (BiOS) mechanism to explain the interannual variability of the ADW outflow. According to the BiOS mechanism (feedback), the North Ionian Gyre circulation is connected to the deep water formation in the Adriatic as follows: when the North Ionian Gyre is cyclonic, saline LIW is advected into the Adriatic, enhancing its deep formation and outflow. This dense water outflows to the flanks of the North Ionian Sea, resulting in deepening of the isopycnals in the flanks region, weakening its cyclonic circulation and eventually reversing the circulation over the North Ionian to become anticyclonic. In turn, this anticyclonic circulation leads to the advection of fresh AW into the Adriatic, diluting its dense water and so the ADW outflow cause the flanks of the North Ionian to become lighter, and thus to reverse the surface pressure gradient back to a cyclonic circulation.

In winter 2012, an intense air-sea heat loss was accounted for highly dense ADW outflow (Bensi et al., 2013; Mihanović et al., 2013) that altered the North Ionian circulation from cyclonic to anticyclonic (Gačić et al., 2014), demonstrating that an external forcing can cause the circulation reversal, interfering (or interacting) with the internal BiOS mechanism. Still, to our knowledge, the BiOS mechanism was not reproduced by general circulation model simulations (Dunić et al., 2016) nor fully explained by conceptual models (Crisciani and Mosetti, 2016; Mosetti, 2016). Dunić et al. (2016) ran an eddy-permitting model of the Adriatic and showed that an interannual variability in ADW formation do exist under realistic forcing, and it is governed by the strengthening and weakening of only a cyclonic circulation of the North Ionian Gyre. Based on a simple dynamical model, Crisciani and Mosetti (2016) suggested that a stochastic resonance mechanism underlies the variability of the North Ionian, BiOS like circulation, and found that the Ionian circulation reversal is driven by a lateral action of surrounding flows rather than by internal feedback between the Ionian and the Adriatic. This result was further supported by general circulation model simulations of the Ionian-Adriatic region (Reale et al., 2016). Furthermore, Reale et al., (2017) showed that the Ionian surface elevation, as an indication of its surface circulation, covaries with the Aegean upper level salinity through an advective signal. Mosetti (2016) showed that the BiOS mechanism resembles the Van der Pol oscillator, thus, an external energy source is necessary to sustain its periodic variability.

Another mechanism explaining the interannul variability of the ADW outflow is the ‘pumping-mechanism’ proposed by Theocharis et al. (2014). In this mechanism, the Aegean and Adriatic Seas receive relatively fresh AW in turn as a function of their role as deep water formation sites. When a sea produces deep water, its overturning circulation is intensified and so it is ‘pumping’ surface AW which stabilizes its water column. The other Sea is then receiving less AW and thus becomes denser until its water column destabilizing and vice versa.

Both the BiOS and the ‘pumping-mechanism’ described above are internal feedbacks and can exist even without the variability of an external forcing. Indeed, studies examining the interannual variability of the Adriatic's main external forcing, i.e., the Bora Wind outbreaks and the Po River discharge, concluded that these affect only the local northern ADW formation variability (Supić and Orlić, 1999; Jeffries and Lee, 2007; Oddo and Guarnieri, 2011), which is a small fraction (about 15%) of the ADW total outflow (Artegiani et al., 1997b; Mantziafou and Lascaratos, 2004, 2008). Furthermore, Oddo and Guarnieri (2011) argued, based on both numerical simulations and direct observations, that even under extreme atmospheric conditions over the Adriatic, no ADW formation processes can occur without the presence of LIW in the Adriatic. Therefore, the study of the response of the ADW outflow to the wind-stress over the Rhodes Gyre, where most of the LIW is generated (Pinardi and Navarra, 1993; Molcard et al., 2002; Pinardi et al., 2015), is important.

A few studies were carried out to investigate the reaction of the EM deep water formation to wind-stress. Samuel et al. (1999) simulated the reaction of the EM overturning circulation to winter wind-stress before and during the EMT. They showed that the path of LIW in the Ionian Sea was different during the two periods. Before the EMT, LIW entered the Adriatic while during the transition it did not, strengthening the role of wind-stress in deep water formation in the EM. However, they used two mean wind-stress fields for the two periods, not taking into account the role of the interannual variability of the wind-stress. Using an oceanic model Molcard et al. (2002) showed that the Mediterranean's general circulation (i.e, its sub-basin scale gyres and boundary currents) response to the wind-stress has an interannual variability that includes the change in phase and amplitude of the seasonal cycle. The northern branch of the Rhodes Gyre, the Asia Minor Current (AMC), was also shown to dynamically respond to the wind-stress (Pinardi and Navarra, 1993; Molcard et al., 2002) and was found to be a coastal downwelling region (Feliks, 1991; Waldman et al., 2018). It was shown that successive winter storms accompanied by intensified wind-stress over Cyprus, resulted in an intense coastal downwelling in the AMC region.

Following the above, the source of the interannual variability of the Eastern Mediterranean Sea circulation is still not fully resolved (Malanotte-Rizzoli et al., 2014, Pinardi et al., 2015). Here we study the interannual variability of the ADW outflow using a fairly realistic general circulation model forced by monthly varying wind-stress and monthly climatological heat and freshwater fluxes. Thus we focus on the effect of the wind-stress variability on the variability of the EM deep water formation, ruling out the effect of interannual variability of heat and freshwater fluxes. We show that the simulated ADW interannual variability is linked to the LIW interannul variability which is controlled, in part, by the wind-stress over the Rhodes Gyre area. The rest of the paper is organized as follows: in Section 2 we shortly present the oceanic model we use and the experiments we conducted with it, in Section 3 we describe the results and we conclude in Section 4.

2. Methodology

We use the Massachusetts Institute of Technology general circulation model (MITgcm, Marshall et al., 1997a, 1997b) to simulate the entire Mediterranean Sea, where the western open boundary is located west of Gibraltar Strait (Fig. 1). We use 22, unevenly spaced, vertical levels located at the following depths: 10, 30, 50, 75, 100, 125, 150, 200, 250, 300, 400, 500, 600, 800, 1000, 1200, 1500, 2000, 2500, 3000, 3500 and 4000 m. This choice enables us to resolve the dynamic of intermediate depths. The horizontal resolution is $1/8° \times 1/8°$ on a spherical grid; a resolution that is equivalent to 14 km in the meridional direction and to 9–12 km in the zonal direction and is fine enough to permit eddy activity. The time step for both tracers and momentum is 1200 s. See Amitai et al. (2017) for more details regarding the MITgcm setting and parametrizations.

The model was initialized with January climatological (averaged over 1987–2014) temperature and salinity fields of Copernicus reanalysis (http://marine.copernicus.eu/) and run for 1500 years until a statistical seasonal steady state was achieved. During this spin-up run, sea surface temperature (SST) and sea surface salinity (SSS) were relaxed toward the monthly averaged climatological SST and SSS of the Copernicus reanalysis with a relaxation time of 8 and 6 days, respectively. Wind-stress forcing was constructed by spatially interpolating the monthly climatology of ERA-Interim wind-stress field (Dee et al.,

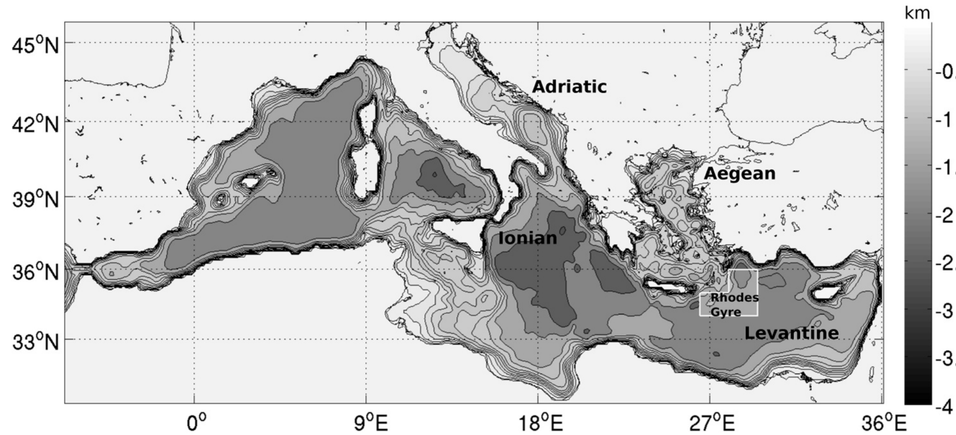

Fig. 1. Model's bathymetry. The main EM basins are specified and the white transparent polygon indicates the Rhodes Gyre area.

2011). Monthly salt/freshwater flux was diagnosed and the simulation continued with mixed surface boundary conditions (of prescribed freshwater flux and relaxation to Copernicus SST) for additional 500 years, to allow the development of natural variability in the simulations (Haney, 1971).

Then, the sea surface was forced by ERA-Interim 1979 wind-stress for 20 years to introduce a realistic momentum forcing to the climatological model. Afterwards, it was forced by monthly means varying ERA-Interim wind-stress (see Fig. 2 for the wind-stress seasonal climatology) for 36 years, between 1979 and 2014; the restored SST and salt/freshwater flux are as in the spin-up run. These surface boundary conditions were chosen to isolate the effect of the wind-stress on the interannual variability of the ADW outflow.

Seasonal averages of the wind-stress plotted overlying the wind-stress curl are presented in Fig. 2. The known bipolar structure of the wind-stress curl over the southern Aegean Sea due to the Etesian winds (Tyrlis and Lelieveld, 2013) is clearly present in summer and autumn months. The positive part of this dipole imposes positive vorticity on the sea surface that drives the permanent cyclonic Rhodes Gyre (Pinardi and Navarra, 1993; Molcard et al., 2002; Pinardi et al., 2015) and its negative part drives the Ierapetra anticyclone (Golnaraghi and Robinson, 1994; Amitai et al., 2010).

To examine the significance of the relationship we found between LIW and ADW formation (Sec. 3), we generated artificial wind-stress fields for a time period of twenty times the original 36 years, i.e., 720 years. The artificial data was generated based on Empirical Orthogonal Function (EOF) analysis of the ERA-Interim wind-stress monthly anomalies. Then, following Alves and Robert (2005), we generated random anomalies field by combining random weighting of the first 50 EOFs (which account for 96% of the variance). The use of spatial EOFs wind patterns is essential to capture realistic surface circulation and hence deep and intermediate water formation regions.

Twenty sets of wind-stress anomalies ($\tau'_{x,y}$), each 36 years long, were created as follows:

$$\tau'_{x,y}(x, y, t) = \sum_{i=1}^{50} R_i P_i(x, y) T_i(t), \tag{1}$$

where $P_i(x, y)$ is the ith EOF, $T_i(t)$ is the corresponding time series and R_i is a Weibull distributed random number normalize to be between zero and one, where the sum of all R_i is equal to one. The Weibull distribution from which all R_i were taken has a shape parameter equals to 0.3 to fit the EOFs eigenvalues distribution. The wind-stress fields that were used to force this simulation were constructed from the artificial anomalies field plus the monthly climatological field such that the mean seasonal cycle is preserved and the interannual variability arise from the anomalies.

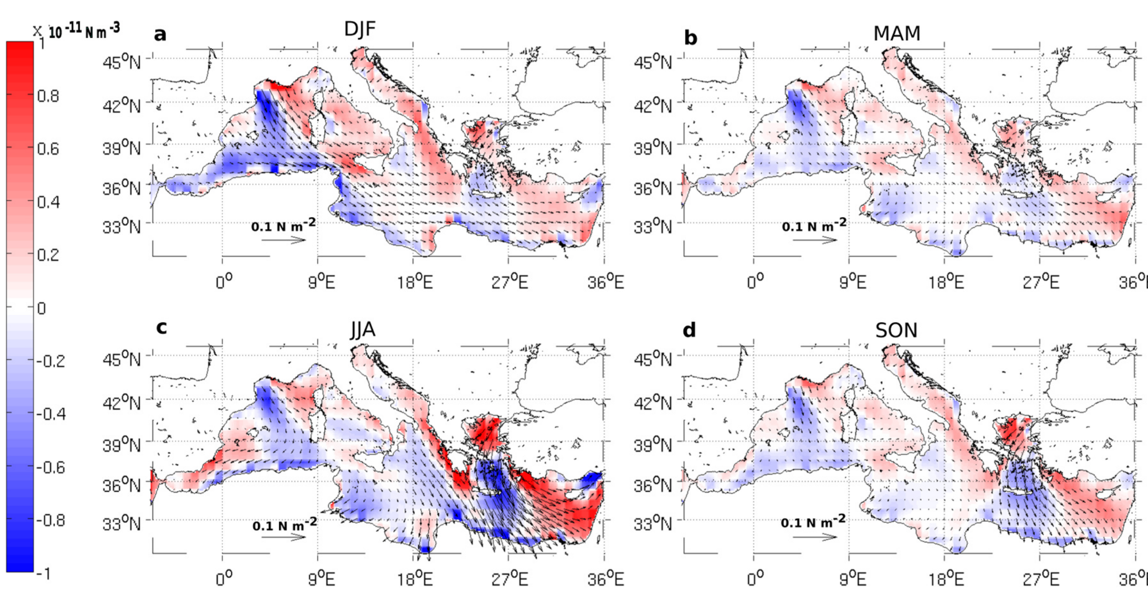

Fig. 2. ERA-Interim climatological wind-stress (arrows) over wind-stress curl (color) in (a) DJF, (b) MAM, (c) JJA and (d) SON. DJF stands for December-January-February and so on.

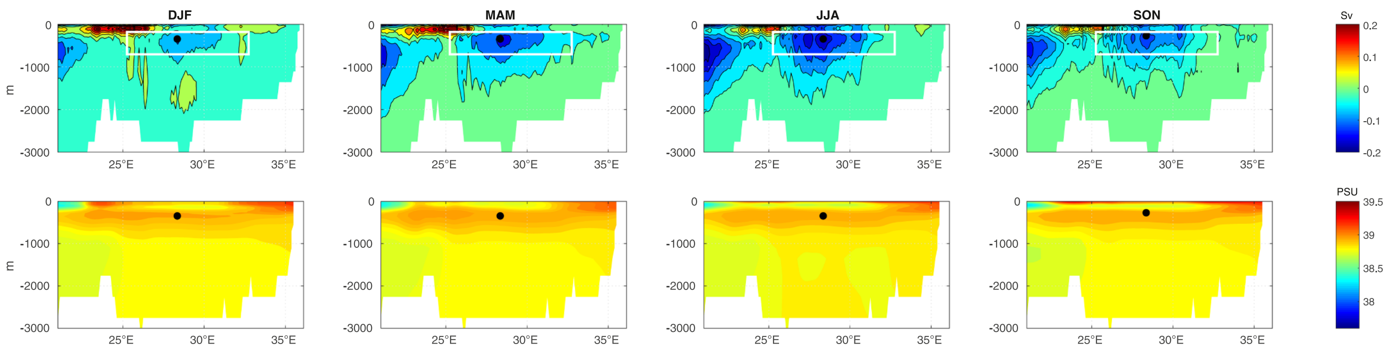

Fig. 3. Seasonal climatology over 36 years of the Levantine zonal overturning circulation streamfunction (upper panels) and of the salinity transect along latitude 34°*N* (lower panels). The white rectangle in the upper panels indicates the region of minimal streamfunction (i.e. clockwise circulation) and the black dot in all panels indicates the actual location of this minimum (which we define as the LIW index).

2.1. Zonal overturning circulation

To characterize the intensity of the formation of LIW we calculated the zonal overturning circulation streamfunction (a meridional integration of the zonal velocity, which is cumulatively integrated from bottom to top) of the entire Leventine basin. We then chose the minimal streamfunction value within the region indicated by the white rectangles shown in the upper panels of Fig. 3. The rectangle was chosen based on the LIW mass location in previous studies (Ovchinnikov and Plakhin, 1984; Lascaratos et al., 1993; Wu and Haines, 1996). This minimum in the center of the streamfunction closed cell represents the intensity of the clockwise overturning circulation associated with the formation and advection of LIW and is defined as the LIW index hereafter (a time series of its annual mean is depict in Fig. 5 as the orange line). We are aware that the overturning circulation is not a direct measure of the LIW sinking (Waldman et al., 2018), however it is directly related to its zonal advection which implies its amount by continuity, hence to its formation intensity .

2.2. PaTATO toolbox

To better understand the variability of ADW outflow under different wind-stress amplitudes, we have conducted a Lagrangian transport analysis using the particle tracking and analysis toolbox (PaTATO) for Matlab (Fredj et al., 2016). Similar to connectivity analysis for ecological purposes (Berline et al., 2014; Rossi et al., 2014; Carlson et al., 2016), we obtained the connectivity between the Adriatic deep layers and the rest of the EM by computing Lagrangian backward-trajectories of 580 particles located deeper than 300 m inside the Adriatic (black squares in Fig. 8) in a 3D, monthly changing, velocity field. The particles were tracked back for four years and a new release was carried out every six months, to allow statistical analysis over a few sets of tracking. We then calculate the percentage of particles from each given source region (as defined by the polygons in Fig. 8 and normalized by the polygon wet area) that reached the deep layers of the Adriatic and the average transit time based on all the sets of backward-trajectories. The entire analysis was carried out for the simulations with ERA-Interim wind-stress (Fig. 8a) and a doubled-amplitude ERA-Interim wind-stress (Fig. 8b).

3. Analysis and results

A seasonal climatology, from the 36 years simulation, of the LIW formation and properties is shown in Fig. 3. The lower panels of Fig. 3 depict a salinity transect along latitude 34°*N* for the sake of example and show that the minimal overturning (black dots in Fig. 3) corresponds to the relatively high salinity values of the LIW ($S \geq 39.00$, Lascaratos et al., 1993; LIWEX Group, 2003). We note that the monthly maximum of LIW index is in September (the monthly time series is not shown here) but the seasonal maximum is in summer (JJA), when the wind-stress amplitude is the largest (Fig. 2c). From observational surveys (LIWEX Group, 2003) and based on the winter temperature that characterizes the LIW (Wüst, 1961; Hecht et al., 1988), it is clear that the LIW formation occurs mainly in winter. Yet, the high LIW index values seen in summer climatology, in our model, can be attributed to the intense wind-stress, suggesting a secondary formation period. Furthermore, Wüst (1961) noted that in summer the LIW westward propagation is more robust than in winter, supporting our result from a zonal streamfunction based index.

An interannual variability in the LIW and in the ADW formation is evident (not shown here but implied by the following calculation) under monthly climatological atmospheric forcing as a consequence of the natural variability of the model. However, forcing the MITgcm with monthly varying ERA-Interim wind-stress result in enhanced variability in the annual anomalies in both the LIW and the ADW formation rates. To quantify this increase, we calculated the standard deviation of the LIW index and ADW outflow time series under climatological (sdt_c) vs. varying (sdt_v) wind-stress forcing and obtained the following

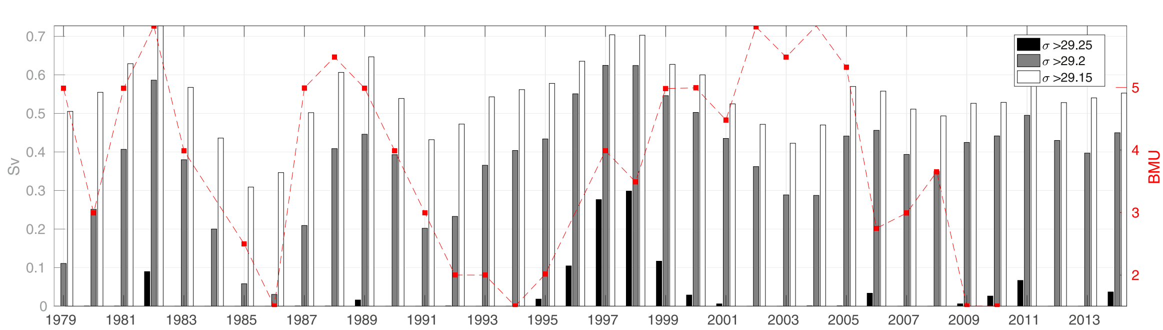

Fig. 4. Time series (1979–2014) of the annual mean outflow through Otranto Strait of the Adriatic for several density thresholds from the model (gray bars) and of the annual mean Best Matching Unit (BMU) from Mihanović et al. (2015).

parameter: $r = (\mathrm{sdt}_v - \mathrm{sdt}_c)/(\mathrm{sdt}_v + \mathrm{sdt}_c)$. The value of this parameter can vary between one, when $\mathrm{sdt}_v \gg \mathrm{sdt}_c$ (e.g., for the wind-stress forcing itself), and minus one, when $\mathrm{sdt}_v \ll \mathrm{sdt}_c$ (i.e., variability is completely attenuated). In our case, the value of r for the LIW index variability is 16% and for the ADW outflow is 29%. This result indicates that the variability of both the LIW and of the ADW formation is increased by the variability of the wind-stress.

The ADW outflow variability is not only enhanced under changing wind-stress forcing, it is also in agreement with observations of the ADW outflow variability in the modeled years. An histogram plot of annual ADW outflow, for different density thresholds, modeled under the realistic wind-surface forcing of ERA-Interim is plotted and compared to observations assembled by Mihanović et al. (2015) in Fig. 4. They examined the interannual variability of the Adriatic intermediate and deep water characteristic by analyzing long-term time series from stations along the central Adriatic Sea and obtained six typical maps of temperature, salinity and dissolved oxygen. Then they identified every observation with the most representative map using the Self-Organizing Maps method and constructed a long-term time series of these maps, i.e., its Best Matching Unit – BMU (Mihanović et al., 2015, Fig. 5). We find similarities between our results and Mihanović et al. (2015) BMUs. For example, Mihanović et al. (2015) identified in 1982 high salinity in the ADW, represented by large BMU, indicating strong outflow that is also evident in our modeled ADW outflow. Another example is the fresh ADW during 1985–1986 as indicated by the characterizing map of Mihanović et al. (2015) and by the relativity weak outflow in our time series. This analogy repeats itself in the high ADW salinity with strong outflow in 1988, 1997–1999 and 2005, and low ADW salinity with weak outflow in 1991–1993 (a period that corresponds to the EMT event). Although there are periods of mismatching (e.g., 2002–2004), the cross-correlation between Mihanović et al. (2015) time series and our ADW outflow (density > 29.2 $\sigma_\theta\,[kg/m^3]$) time series, on an interannual basis, yields $R = 0.9$. Periods of mismatching between the observed and modeled ADW outflow are presumably a result of the uncounted variability in heat and freshwater fluxes.

The interannual time series of the simulated ADW outflow and the LIW index (as reflected by the minimal streamfunction, see Fig. 3) over 1979–2014 are shown in Fig. 5a, where the main trends are in a good agreement. Note that the values of both the ADW outflow and the LIW index in the time series are negative since the ADW outflow is southward and the LIW streamfunction cell is clockwise; i.e., minimal values stand for stronger formation rate. A lagged cross-correlation between the year-to-year differences in the LIW index and in the ADW outflow was calculated since we argue that a change in one parameter (the LIW index) can lead to a change in the other parameter (the ADW outflow). We found a correlation coefficient of $R = 0.4$ at a negative time lag of one year and of $R = 0.28$ in a zero time lag (both distinctly higher than in any other time lag and with p-value smaller than 0.05). The correlation coefficients between the anomalies from the annual means of the LIW index and the ADW outflow are even higher ($R = 0.55$ and $R = 0.46$ at a negative one year time lag and zero time lag, respectively; p-value <0.05). Thus, the minimal streamfunction associated with LIW formation precedes the ADW outflow by up to one year; this is in a fair agreement with the ARGO based observations of the LIW travel time to the Adriatic (~ 1.5 years) made by Bensi et al. (2016) and calculated in an OGCM (Amitai et al., 2017; Reale et al., 2017).

The significance of the correlation coefficients reported here were quantified using surrogate data test in which the two times series where shuffled and the correlation coefficients were re-calculated; this procedure was repeated 100 times and based on these surrogate time series we estimated the p-value.

As mentioned in Section 2, to gain better statistical performance, we also computed the LIW formation rate (represented by the LIW index) and ADW outflow based on artificially generated wind-stress time series. The time series of both the LIW index and the ADW outflow (Fig. 5b) shows centennial variability. A cross-correlation between the annual year-to-year differences in LIW index and in the ADW outflow when using 720 years of artificial wind-stress (as described in Section 2) shows that the largest correlation coefficient ($R = 0.33$) is at a negative one year time lag and similar ($R = 0.27$) at a zero time lag (p-value < 0.05 for both). These correlation coefficients are distinctly higher than in other lags and strengthening the results that LIW formation precedes the ADW outflow by up to one year in our simulation. The correlation coefficient between anomalies from the annual means of the LIW streamfunction and the ADW outflow is $R \cong 0.8$ in both a negative one year and a zero time lags. When dividing the 720 years time series to twenty sets of 36 years (that are based on the EOFs), we found that in a negative lag of one year and in zero time lag the average of twenty correlation coefficients is $R \cong 0.5$ as in the simulation with ERA-Interim forcing.

A map of cross-correlation coefficients between the time series of the annual mean wind-stress (amplitude and curl) in every grid point and the annual mean of the LIW index time series is presented in Fig. 6. It shows that the cross-correlation coefficients between the LIW index and wind-stress amplitude (Fig. 6a) in the Rhodes Gyre area (indicated by the white polygon in Fig. 1) is $R = -0.65$; p-value < 0.05. The sign of R is negative since a strong (positive anomaly) wind-stress driving the Rhodes Gyre strengthens the clockwise (negative sign) vertical circulation of the LIW. The correlation between the LIW index and the wind-stress curl (Fig. 6b) over the Rhodes Gyre has the spatial dipole pattern

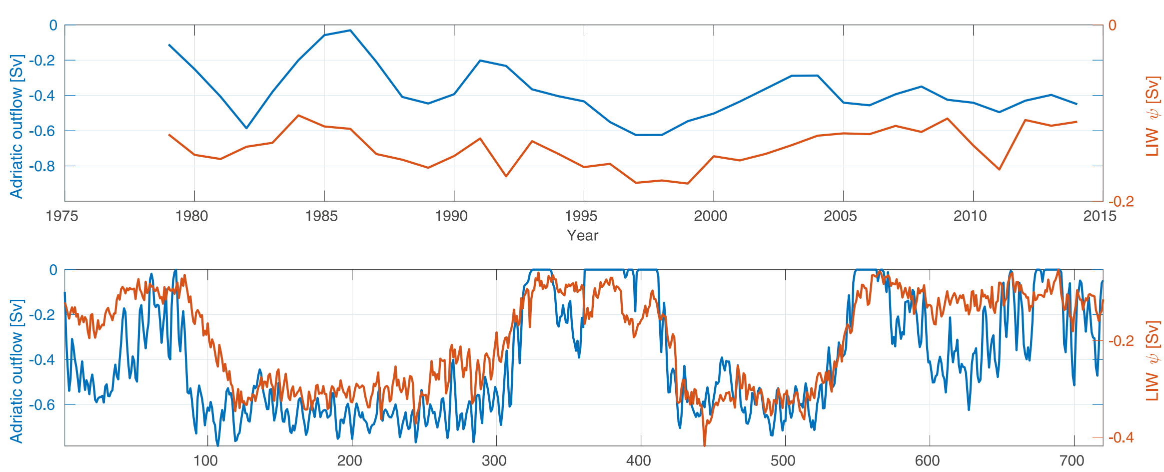

Fig. 5. Time series of the annual LIW intensity and the ADW outflow of water denser than 29.2 $\sigma_\theta\,[kg/m^3]$ over (a) 36 years between 1979 and 2014 and (b) 720 years with artificial wind-stress as described in Sec. 2. The values are negative since the ADW outflow is southward and the LIW streamfunction cell is clockwise.

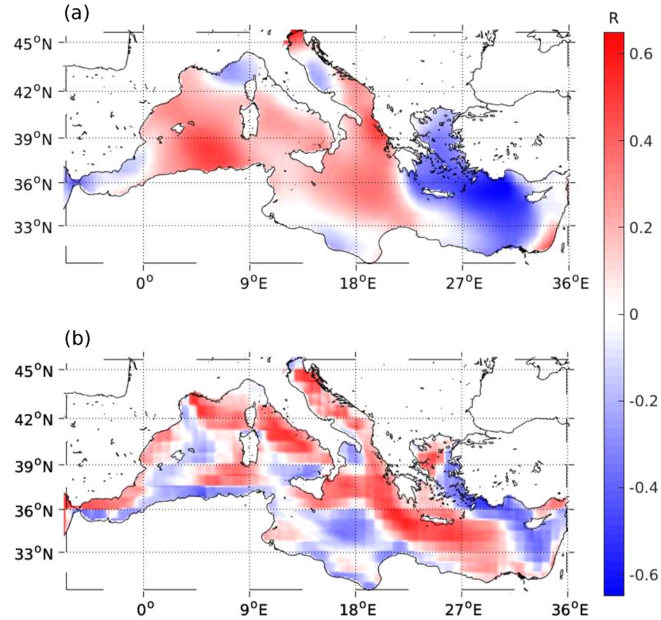

Fig. 6. Cross-correlation coefficients map between the time series of wind-stress (a) amplitude and (b) curl in each grid point of the model and the time series of the LIW index over the 36 years simulation period (1979–2014).

evident in the wind-stress curl maps (Fig. 2). In its positive part the correlation coefficient is also R = −0.65; p-value < 0.05. These high correlation coefficients, appear in both maps together, highlight the connection between the LIW index interannual variability and the wind-stress over the Rhodes Gyre interannual variability. Still, further observational work is needed to find the contribution of each wind-stress parameter (the curl and the amplitude) to the LIW formation.

3.1. Wind-stress amplitude analysis

To further study the influence of the wind-stress amplitude on the LIW intensity and hence on the ADW outflow, we performed a set of simulations with the same spatial pattern of 36 years of ERA-Interim wind-stress fields but with amplitude that ranges between 0.5 and 2 times the control run. More specifically, the wind-stress field over the entire Mediterranean was multiplied by a factor between 0.5 and 2 (total of seven simulations). Each simulation started with a run of 200 years with the wind-stress of 1979 (as another spin-up run) multiplied by a factor and then run for 36 years with the wind-stress of 1979–2014 multiplied by the same factor.

The northern branch of the Rhodes Gyre, the AMC, responds approximately linearly to wind-stress amplitude (Fig. 7a). This result is expected as the Rhodes Gyre circulation depends on the wind-stress intensity and its curl (Molcard et al., 2002), which also increases as a function of the wind-stress amplitude. Slightly stronger LIW index (Fig. 7b) appears above wind-stress amplitude multiplied by 1.5 and the mean inflow through Sicily Strait (Fig. 7d) does not show a distinct trend. However, we note that the interannual variability (shown by the error bars in Fig. 7) of the maximal water inflow from the Sicily Strait (mainly of fresh AW) is larger when the wind-stress amplitude is higher. Meaning that pulses of fresh water from the Western Mediterranean into the Eastern Mediterranean are more intense under stronger wind-stress.

The mean ADW outflow dependence on the wind-stress amplitude is more complex, it has a maximal value under present day wind-stress, i.e., $1 \times \tau$ (Fig. 7c). The results indicate that under low wind-stress amplitude there is no ADW formation and it is weaker when the wind-stress is stronger than the present wind-stress field. No ADW outflow under low wind-stress amplitude can be attributed to insufficient advection of saline water from the Levantine to the Adriatic as can be seen in the low values of the AMC magnitude (Fig. 7a) under low wind-stress amplitude. Weak ADW outflow under high wind-stress amplitude may

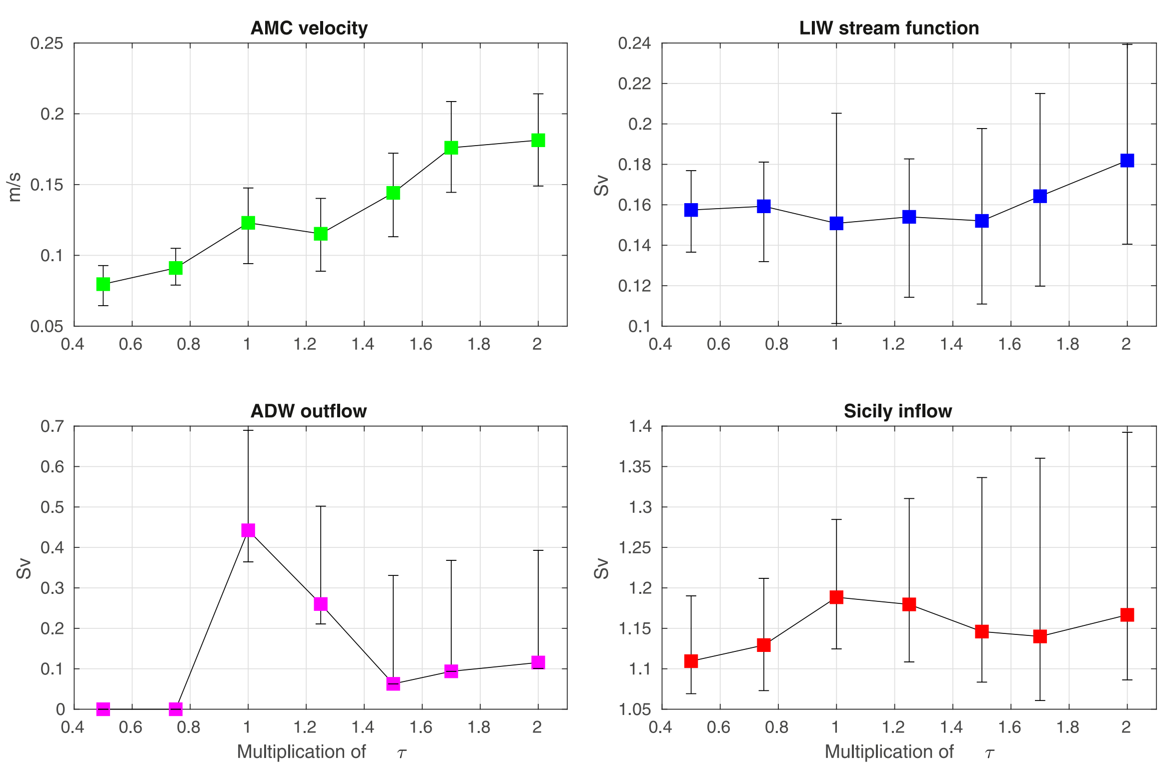

Fig. 7. (a) Mean velocity over the AMC region, (b) mean LIW index, (c) mean ADW outflow and (d) mean inflow from Sicily calculated from a set of seven simulations (including the control run), 36 years long each, with a different factor multiplying the ERA-Interim wind-stress forcing. The error bars are one standard deviation of the annual maximum and minimum in each 36 years simulation.

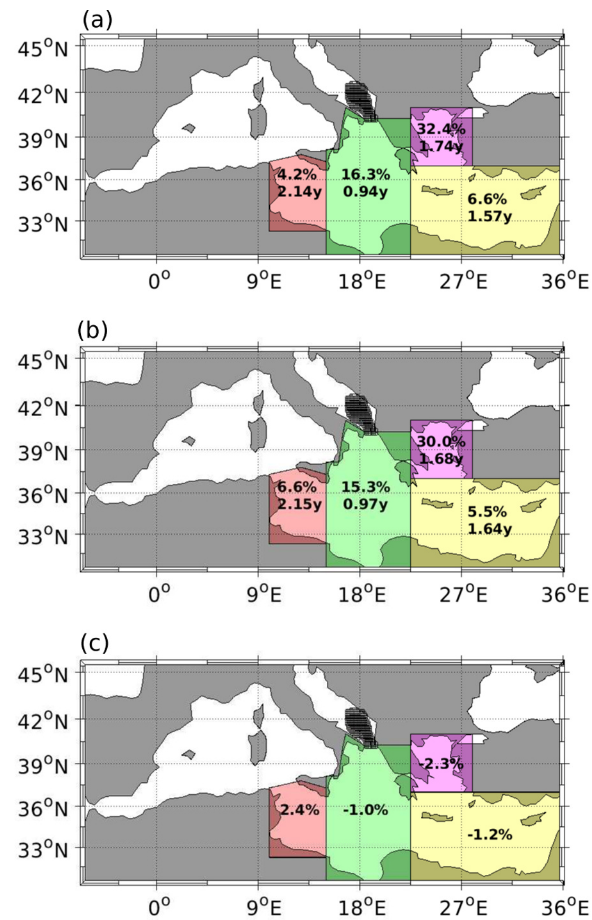

Fig. 8. Connection percentages, or the percentage of particles from each polygon, normalized by the polygon wet area, that reached the deep levels of the Adriatic Sea (≤ 300 m; marked in black squares) and their average transit times under (a) present day ERA-Interim wind-stress, under (b) 2 times ERA-Interim wind-stress forcing, and (c) the difference between them (i.e. (b) minus (a)).

be a consequence of stronger pulses of freshwater advected from the Western Mediterranean, as can be seen from the high variability of Sicily inflow (Fig. 7d) under stronger wind-stress. Note that the wind-stress spatial pattern is mostly southward and eastward. The fresher water coming from the north and from the west can stabilize the Adriatic's water column and thus can lead to a reduced ADW formation. We examine this idea in the next section.

3.2. Lagrangian transport

Examining the connectivity maps of the different source region to the Adriatic deep layers, we identify some features of ADW main sources. The Ionian (green polygon) is the fastest supplier to the ADW as it is in a direct connection with the Adriatic. Water from the Aegean Sea (magenta polygon), which passes trough the Levantine basin provides high percentage of its water to the Adriatic with respect to its size (the percentage are normalized to each polygon area to be able to compare between the source regions). This result agrees with the reported connection between the Aegean and the Adriatic Seas's overturning circulation (Theocharis et al., 2014; Velaoras et al., 2014; Amitai et al., 2017; Reale et al., 2017). The Sicily Straits (red polygon) has the longest average transit time to the deep Adriatic (~ 2.1 years) and supplies only ~ 4% of it, under unchanged ERA-Interim wind-stress forcing (Fig. 8a). However, under wind-stress forcing amplitude multiplied by 2 (Fig. 8b) the water supply from the Sicily Straits to the ADW is rising by more than 50% of its original value while the supply from other regions is reduced (Fig. 8c). Calculating similar connectivity maps with wind-stress forcing amplitude multiplied by 1.5 and by 1.7 (not shown here) we get the same result of increased water supply from the west and decreased water supply from the east, compared to the unchanged ERA-Interim wind-stress forcing.

We suggest that this result support our secondary hypothesis regarding the ADW relationship with high wind-stress amplitude over the entire Mediterranean. It seems that both the advected LIW and the advected water from Sicily Strait can dictate the ADW formation, according to their relative strength and pathway at different wind-stress amplitude. This finding has a resemblance to the reported BiOS mechanism (Gačić et al., 2010), but externally driven.

4. Conclusions

The main result of this work is the connection between the wind-stress regime and the deep water formation in the Adriatic. By forcing an oceanic general circulation model of the Mediterranean Sea with 1979–2014 ERA-Interim wind-stress but with the climatological (monthly averaged over 1987–2014) heat and freshwater fluxes we reproduce the interannual variability of the ADW formation in accordance with observations. We found high correlations between the wind-stress magnitude and curl over the Rhodes Gyre area and the LIW intensity on the one hand and between the LIW intensity and the ADW outflow on the other hand.

We have found up to one year lagged correlations, in agreement with observation (Bensi et al., 2016) and multi-model (Reale et al., 2017) results, according to which the LIW intensity leads the ADW outflow by several months. It essentially implies that the wind-stress affects the formation of the LIW formation, which later affects the deep water formation in the Adriatic Sea. Since ADW formation is activated by sub-surface preconditioning and the LIW course into the Adriatic takes a few months according to our model, the use of monthly (instead of synoptic) wind stress forcing is valid.

To better establish the above connection we have performed 720 years simulation that is forced by artificially perturbed wind-stress field. We found similar high correlations between the LIW intensity and the ADW outflow. In addition, this long-term simulation indicates variability on centennial time scale of both the LIW and the ADW formation.

When the wind-stress amplitude is between 0.5 and 2 times the original ERA-Interim magnitude, the AMC intensity increases approximately linearly as a function of the wind-stress amplitude. However, the ADW outflow is maximal when the wind-stress is as present day. This implies a different balance between the LIW water mass and the fresh AW mass entering the EM from Sicily Strait under stronger than present wind-stress amplitude.

By conducting a Lagrangian transport analysis between the deep levels of the Adriatic and the different regions of the EM, we confirm that under high wind-stress amplitude we get a different balance between the LIW water mass and the freshwater mass entering the EM from Sicily Strait. This result is significant under the prediction that the average wind speed will increase in some regions of the Mediterranean under IPCC (Intergovernmental Panel on Climate Change) scenarios (Goodess et al., 2013).

To summarize, we found that the ADW outflow is effected by the LIW formation strength that is also a function of the wind-stress magnitude over the Rhodes Gyre area in the present wind-stress regime. Our results support former studies connecting the wind-stress to the LIW formation, nevertheless, we show for the first time that there is a remote affect of the wind-stress on the ADW interannual variability.

Acknowledgments

We are grateful to Erick Fredj and Daniel F. Carlson for providing the codes for the Lagrangian transport analysis. We thank Hrvoje Mihanović for sharing his BMU time series with us. Hezi Gildor and Yosef Ashkenazy thank the Israeli Ministry of Science and Italian Ministry of Foreign Affairs. Yael Amitai was partially supported by a fellowship from the Mediterranean Sea Research Center of Israel.

References

Alves, O., Robert, C., 2005. Tropical Pacific Ocean model error covariances from Monte Carlo simulations. Q. J. R. Meteorol. Soc. 131 (613), 3643–3658. https://doi.org/10.1256/qj.05.113.
Amitai, Y., Ashkenazy, Y., Gildor, H., 2017. Multiple equilibria and overturning variability of the Aegean-Adriatic Seas. Glob. Planet. Change 151, 49–59. https://doi.org/10.1016/j.gloplacha.2016.05.004.
Amitai, Y., Lehahn, Y., Lazar, A., Heifetz, E., 2010. Surface circulation of the eastern Mediterranean Levantine basin: insights from analyzing 14 years of satellite altimetry data. J. Geophys. Res.: Oceans 115 (C10). https://doi.org/10.1029/2010JC006147.
Artegiani, A., Paschini, E., Russo, A., Bregant, D., Raicich, F., Pinardi, N., 1997a. The Adriatic Sea general circulation. Part I: air-sea interactions and water mass structure. J. Phys. Oceanogr. 27 (8), 1492–1514. https://doi.org/10.1175/1520-0485(1997)027.
Artegiani, A., Paschini, E., Russo, A., Bregant, D., Raicich, F., Pinardi, N., 1997b. The Adriatic Sea general circulation. Part II: baroclinic circulation structure. J. Phys. Oceanogr. 27 (8), 1515–1532. https://doi.org/10.1175/1520-0485(1997)027.
Bensi, M., Cardin, V., Rubino, A., Notarstefano, G., Poulain, P.M., 2013. Effects of winter convection on the deep layer of the Southern Adriatic Sea in 2012. J. Geophys. Res.: Oceans 118 (11), 6064–6075. https://doi.org/10.1002/2013JC009432.
Bensi, M., Velaoras, D., Meccia, V.L., Cardin, V., 2016. Effects of the Eastern Mediterranean Sea circulation on the thermohaline properties as recorded by fixed deep-ocean observatories. Deep Sea Res. Part I: Oceanogr. Res. Pap. 112, 1–13. https://doi.org/10.1016/j.dsr.2016.02.015.
Berline, L., Rammou, A.-M., Doglioli, A., Molcard, A., Petrenko, A., 2014. A connectivity-based eco-regionalization method of the Mediterranean Sea. PLoS One 9 (11), e111978. https://doi.org/10.1016/j.dsr.2016.02.015.
Cardin, V., Bensi, M., Pacciaroni, M., 2011. Variability of water mass properties in the last two decades in the South Adriatic Sea with emphasis on the period 2006–2009. Cont. Shelf Res. 31 (9), 951–965. https://doi.org/10.1016/j.csr.2011.03.002.
Cardin, V., Civitarese, G., Hainbucher, D., Bensi, M., Rubino, A., 2015. Thermohaline properties in the Eastern Mediterranean in the last three decades: is the basin returning to the pre-EMT situation? Ocean Sci. 11 (1), 391–423. https://doi.org/10.5194/os-11-53-2015.
Carlson, D.F., Griffa, A., Zambianchi, E., Suaria, G., Corgnati, L., Magaldi, M.G., Poulain, P.-M., Russo, A., Bellomo, L., Mantovani, C., et al., 2016. Observed and modeled surface Lagrangian transport between coastal regions in the Adriatic Sea with implications for marine protected areas. Cont. Shelf Res. 118, 23–48. https://doi.org/10.1016/j.csr.2016.02.012.
Chiggiato, J., Schroeder, K., Trincardi, F., 2016. Cascading dense shelf-water during the extremely cold winter of 2012 in the Adriatic, Mediterranean Sea: formation, flow, and seafloor impact. Mar. Geol. 375, 1–4. https://doi.org/10.1016/j.margeo.2016.03.002.
Crisciani, F., Mosetti, R., 2016. Is the bimodal oscillating Adriatic-Ionian circulation a stochastic resonance? Boll. Geofis. Teor. Ed. Appl. 57 (3), 275–285. https://doi.org/10.4430/bgta0176.
Dee, D.P., Uppala, S.M., Simmons, A.J., Berrisford, P., Poli, P., Kobayashi, S., Andrae, U., Balmaseda, M.A., Balsamo, G., Bauer, P., Bechtold, P., Beljaars, A.C.M., van de Berg, L., Bidlot, J., Bormann, N., Delsol, C., Dragani, R., Fuentes, M., Geer, A.J., Haimberger, L., Healy, S.B., Hersbach, H., Hólm, E.V., Isaksen, L., Kållberg, P., Köhler, M., Matricardi, M., McNally, A.P., Monge-Sanz, B.M., Morcrette, J.-J., Park, B.-K., Peubey, C., de Rosnay, P., Tavolato, C., Thépaut, J.-N., Vitart, F., 2011. The ERA-Interim reanalysis: configuration and performance of the data assimilation system. Q. J. R. Meteorol. Soc. 137 (656), 553–597. https://doi.org/10.1002/qj.828.
Dunić, N., Vilibić, I., Šepić, J., Somot, S., Sevault, F., 2016. Dense water formation and BiOS-induced variability in the Adriatic Sea simulated using an ocean regional circulation model. Clim. Dyn. 1–26. https://doi.org/10.1007/s00382-016-3310-5.
Feliks, Y., 1991. Downwelling along the northeastern coasts of the eastern Mediterranean. J. Phys. Oceanogr. 21 (4), 511–526. https://doi.org/10.1175/1520-0485(1991)021.
Fredj, E., Carlson, D.F., Amitai, Y., Gozolchiani, A., Gildor, H., 2016. The particle tracking and analysis toolbox (PaTATO) for Matlab. Limnol. Oceanogr.: Methods 14 (9), 586–599. https://doi.org/10.1002/lom3.10114.
Gačić, M., Borzelli, G.L.E., Civitarese, G., Cardin, V., Yari, S., 2010. Can internal processes sustain reversals of the ocean upper circulation? The Ionian Sea example. Geophys. Res. Lett. 37 (9). https://doi.org/10.1029/2010GL043216.
Gačić, M., Civitarese, G., Kovačević, V., Ursella, L., Bensi, M., Menna, M., Cardin, V., Poulain, P.-M., Cosoli, S., Notarstefano, G., Pizzi, C., 2014. Extreme winter 2012 in the Adriatic: an example of climatic effect on the BiOS rhythm. Ocean Sci. 10 (3), 513–522. https://doi.org/10.5194/os-10-513-2014.
Golnaraghi, M., Robinson, A.R., 1994. Dynamical studies of the Eastern Mediterranean circulation. In: Ocean Processes in Climate Dynamics: Global and Mediterranean Examples. Springer, pp. 395–406.
Goodess, C.M., Agnew, M.D., Giannakopoulos, C., Hemming, D., Salem, S.B., Bindi, M., Bradai, M.N., Congedi, L., Dibari, C., El-Askary, H., et al., 2013. Integration of the climate impact assessments with future projections. In: Regional Assessment of Climate Change in the Mediterranean. Springer, pp. 105–162.
Gunduz, M., Dobricic, S., Oddo, P., Pinardi, N., Guarnieri, A., 2013. Impact of Levantine Intermediate Water on the interannual variability of the Adriatic Sea based on simulations with a fine resolution ocean model. Ocean Model. 72, 253–263. https://doi.org/10.1016/j.ocemod.2013.10.002.
Haney, R.L., 1971. Surface thermal boundary condition for ocean circulation models. J. Phys. Oceanogr. 1 (4), 241–248. https://doi.org/10.1175/1520-0485(1971)001.
Hecht, A., Pinardi, N., Robinson, A.R., 1988. Currents, water masses, eddies and jets in the Mediterranean Levantine Basin. J. Phys. Oceanogr. 18 (10), 1320–1353. https://doi.org/10.1175/1520-0485(1988)018.
Jeffries, M.A., Lee, C.M., 2007. A climatology of the northern Adriatic Sea's response to bora and river forcing. J. Geophys. Res.: Oceans 112 (C3). https://doi.org/10.1029/2006JC003664.
Klein, B., Roether, W., Civitarese, G., Gacic, M., Manca, B.B., D'Alcala, M.R., 2000. Is the Adriatic returning to dominate the production of Eastern Mediterranean deep water? Geophys. Res. Lett. 27 (20), 3377–3380. https://doi.org/10.1029/2000GL011620.
Klein, B., Roether, W., Manca, B., 1999. The large deep water transient in the Eastern Mediterranean. Deep Sea Res. Part I: Oceanogr. Res. Pap. 46 (1999), 371–414. https://doi.org/10.1016/S0967-0637(98)00075-2.
Korres, G., Pinardi, N., Lascaratos, A., 2000. The ocean response to low-frequency interannual atmospheric variability in the Mediterranean Sea. Part I: sensitivity experiments and energy analysis. J. Clim. 13 (4), 705–731. https://doi.org/10.1175/1520-0442(2000)013.
Lascaratos, A., Williams, R.G., Tragou, E., 1993. A mixed-layer study of the formation of Levantine Intermediate Water. J. Geophys. Res.: Oceans 98 (C8), 14739–14749. https://doi.org/10.1029/93JC00912.
LIWEX Group, 2003. The Levantine intermediate water experiment (LIWEX) group: Levantine basin – a laboratory for multiple water mass formation processes. J. Geophys. Res.: Oceans 108 (C9). https://doi.org/10.1029/2002JC001643.
Malanotte-Rizzoli, P., Font, J., García-Ladona, E., Pascual, A., Tintoré, J., Triantafyllou, G., 2014. Physical forcing and physical/biochemical variability of the Mediterranean Sea: a review of unresolved issues and directions for future research. Ocean Sci. 10 (3), 281–322. https://doi.org/10.5194/os-10-281-2014.
Malanotte-Rizzoli, P., Manca, B.B., d'Alcalà, M.R., Theocharis, A., Bergamasco, A., Bregant, D., Budillon, G., Civitarese, G., Georgopoulos, D., Michelato, A., et al., 1997. A synthesis of the Ionian Sea hydrography, circulation and water mass pathways during POEM-Phase I. Prog. Oceanogr. 39 (3), 153–204. https://doi.org/10.1016/S0079-6611(97)00013-X.
Malanotte-Rizzoli, P., Manca, B.B., D'Alcala, M.R., Theocharis, A., Brenner, S., Budillon, G., Ozsoy, E., 1999. The Eastern Mediterranean in the 80s and in the 90s: the big transition in the intermediate and deep circulations. Dyn. Atmos. Oceans 29 (2–4), 365–395. https://doi.org/10.1016/S0377-0265(99)00011-1.
Manca, B.B., Budillon, G., Scarazzato, P., Ursella, L., 2003. Evolution of dynamics in the eastern Mediterranean affecting water mass structures and properties in the Ionian and Adriatic Seas. J. Geophys. Res.: Oceans 108 (C9). https://doi.org/10.1029/2002JC001664.
Mantziafou, A., Lascaratos, A., 2004. An eddy resolving numerical study of the general circulation and deep-water formation in the Adriatic Sea. Deep Sea Res. Part I: Oceanogr. Res. Pap. 51 (7), 921–952. https://doi.org/10.1016/j.dsr.2004.03.006.
Mantziafou, A., Lascaratos, A., 2008. Deep-water formation in the Adriatic Sea: interannual simulations for the years 1979–1999. Deep Sea Res. Part I: Oceanogr. Res. Pap. 55 (11), 1403–1427. https://doi.org/10.1016/j.dsr.2008.06.005.
Marshall, J., Adcroft, A., Hill, C., Perelman, L., Heisey, C., 1997a. A finite-volume, incompressible Navier Stokes model for studies of the ocean on parallel computers. J. Geophys. Res.: Oceans 102, 5753–5766. https://doi.org/10.1029/96JC02775.
Marshall, J., Hill, C., Perelman, L., Adcroft, A., 1997b. Hydrostatic, quasi-hydrostatic, and nonhydrostatic ocean modeling. J. Geophys. Res.: Oceans 102, 5733–5752. https://doi.org/10.1029/96JC02776.
Mihanović, H., Vilibić, I., Carniel, S., Tudor, M., Russo, A., Bergamasco, A., Bubić, N., Ljubešić, Z., Viličić, D., Boldrin, A., Malačič, V., Celio, M., Comici, C., Raicich, F., 2013. Exceptional dense water formation on the Adriatic shelf in the winter of 2012. Ocean Sci. 9 (3), 561–572. https://doi.org/10.5194/os-9-561-2013.
Mihanović, H., Vilibić, I., Dunić, N., Šepić, J., 2015. Mapping of decadal middle Adriatic oceanographic variability and its relation to the BiOS regime. J. Geophys. Res.: Oceans 120 (8), 5615–5630. https://doi.org/10.1002/2015JC010725.
Molcard, A., Pinardi, N., Iskandarani, M., Haidvogel, D., 2002. Wind driven general circulation of the Mediterranean Sea simulated with a Spectral Element Ocean Model. Dyn. Atmos. Oceans 35 (2), 97–130. https://doi.org/10.1016/S0377-0265(01)00080-X.
Mosetti, R., 2016. The theory of non-linear oscillator applied to the bios mechanism. ArXiv e-prints: arXiv:1612.05254.
Oddo, P., Guarnieri, A., 2011. A study of the hydrographic conditions in the Adriatic Sea from numerical modelling and direct observations (2000–2008). Ocean Sci. 7 (5), 549–567. https://doi.org/10.5194/os-7-549-2011.
Ovchinnikov, I., Zats, V., Krivosheya, V., Udodov, A., 1985. Formation of deep eastern Mediterranean waters in the Adriatic Sea. Oceanology 25, 704–707.
Ovchinnikov, I.M., Plakhin, A., 1984. Formation of the intermediate waters of the Mediterranean Sea in the Rhodes cyclonic gyre. Oceanology 24, 317–319.
Pinardi, N., Navarra, A., 1993. Baroclinic wind adjustment processes in the Mediterranean Sea. Deep Sea Res. Part II: Top. Stud. Oceanogr. 40 (6), 1299–1326. https://doi.org/10.1016/0967-0645(93)90071-T.
Pinardi, N., Zavatarelli, M., Adani, M., Coppini, G., Fratianni, C., Oddo, P., Simoncelli, S., Tonani, M., Lyubartsev, V., Dobricic, S., Bonaduce, A., 2015. Mediterranean Sea large-scale low-frequency ocean variability and water mass formation rates from 1987 to 2007: a retrospective analysis. Prog. Oceanogr. 132, 318–332. https://doi.org/10.1016/j.pocean.2013.11.003.
Querin, S., Cossarini, G., Solidoro, C., 2013. Simulating the formation and fate of dense

water in a midlatitude marginal sea during normal and warm winter conditions. J. Geophys. Res.: Oceans 118 (2), 885–900. https://doi.org/10.1002/jgrc.20092.

Reale, M., Crise, A., Farneti, R., Mosetti, R., 2016. A process study of the Adriatic-Ionian System baroclinic dynamics. J. Geophys. Res.: Oceans 121 (8), 5872–5887. https://doi.org/10.1002/2016JC011763.

Reale, M., Salon, S., Crise, A., Farneti, R., Mosetti, R., Sannino, G., 2017. Unexpected covariant behavior of the aegean and ionian seas in the period 1987–2008 by means of a nondimensional sea surface height index. J. Geophys. Res.: Oceans 122 (10), 8020–8033. https://doi.org/10.1002/2017JC012983.

Robinson, A., Malanotte-Rizzoli, P., Hecht, A., Michelato, A., Roether, W., Theocharis, A., Ünlüata, Ü., Pinardi, N., Artegiani, A., Bergamasco, A., Bishop, J., Brenner, S., Christianidis, S., Gacic, M., Georgopoulos, D., Golnaraghi, M., Hausmann, M., Junghaus, H.-G., Lascaratos, A., Latif, M., Leslie, W., Lozano, C., Oguz, T., Özsoy, E., Papageorgiou, E., Paschini, E., Rozentroub, Z., Sansone, E., Scarazzato, P., Schlitzer, R., Spezie, G.-C., Tziperman, E., Zodiatis, G., Athanassiadou, L., Gerges, M., Osman, M., 1992. General circulation of the Eastern Mediterranean. Earth-Sci. Rev. 32 (4), 285–309. https://doi.org/10.1016/0012-8252(92)90002-B.

Roether, W., Manca, B.B., Klein, B., Bregant, D., Georgopoulos, D., Beitzel, V., Kovačević, V., Luchetta, A., 1996. Recent changes in eastern Mediterranean deep waters. Science 271 (5247), 333–335. https://doi.org/10.1126/science.271.5247.333.

Rossi, V., Ser-Giacomi, E., López, C., Hernández-García, E., 2014. Hydrodynamic provinces and oceanic connectivity from a transport network help designing marine reserves. Geophys. Res. Lett. 41 (8), 2883–2891. https://doi.org/10.1002/2014GL059540.

Russo, A., Artegiani, A., 1996. Adriatic Sea hydrography. Sci. Mar. 60, 33–43.

Samuel, S., Haines, K., Josey, S., Myers, P.G., 1999. Response of the Mediterranean Sea thermohaline circulation to observed changes in the winter wind stress field in the period 1980–1993. J. Geophys. Res.: Oceans 104 (C4), 7771–7784. https://doi.org/10.1029/1998JC900130.

Supić, N., Orlić, M., 1999. Seasonal and interannual variability of the northern Adriatic surface fluxes. J. Mar. Syst. 20 (1–4), 205–229. https://doi.org/10.1016/S0924-7963(98)00083-9.

Theocharis, A., Krokos, G., Velaoras, D., Korres, G., 2014. An internal mechanism driving the alternation of the Eastern Mediterranean dense/deep water sources. Mediterr. Sea: Tempo. Var. Spat. Patterns. https://doi.org/10.1002/9781118847572.ch8.

Tyrlis, E., Lelieveld, J., 2013. Climatology and dynamics of the summer etesian winds over the Eastern Mediterranean. J. Atmos. Sci. 70 (11), 3374–3396. https://doi.org/10.1175/JAS-D-13-035.1.

Velaoras, D., Krokos, G., Nittis, K., Theocharis, A., 2014. Dense intermediate water outflow from the Cretan Sea: a salinity driven, recurrent phenomenon, connected to thermohaline circulation changes. J. Geophys. Res.: Oceans 119 (8), 4797–4820. https://doi.org/10.1002/2014JC009937.

Verri, G., Pinardi, N., Oddo, P., Ciliberti, S.A., Coppini, G., 2018. River runoff influences on the Central Mediterranean overturning circulation. Clim. Dyn. 50 (5–6), 1675–1703. https://doi.org/10.1007/s00382-017-3715-9.

Vervatis, V.D., Sofianos, S.S., Skliris, N., Somot, S., Lascaratos, A., Rixen, M., 2013. Mechanisms controlling the thermohaline circulation pattern variability in the Aegean-Levantine region. A hindcast simulation (1960–2000) with an eddy resolving model. Deep Sea Res. Part I: Oceanogr. Res. Pap. 74, 82–97. https://doi.org/10.1016/j.dsr.2012.12.011.

Waldman, R., Brüggemann, N., Bosse, A., Spall, M., Somot, S., Sevault, F., 2018. Overturning the Mediterranean thermohaline circulation. Geophys. Res. Lett. https://doi.org/10.1029/2018GL078502.

Wu, P., Haines, K., 1996. Modeling the dispersal of Levantine Intermediate Water and its role in Mediterranean deep water formation. J. Geophys. Res.: Oceans 101, 6591–6607. https://doi.org/10.1029/95JC03555.

Wüst, G., 1961. On the vertical circulation of the Mediterranean Sea. J. Geophys. Res. 66 (10), 3261–3271. https://doi.org/10.1029/JZ066i010p03261.